

# An Ultra-Wide-Band Tightly Coupled Dipole Reflectarray Antenna

Wenting Li<sup>1</sup>, Steven Gao, *Senior Member, IEEE*, Long Zhang<sup>2</sup>, Qi Luo<sup>3</sup>, *Member, IEEE*,  
and Yuanming Cai<sup>4</sup>, *Member, IEEE*

**Abstract**—A novel ultra-wide-band tightly coupled dipole reflectarray (TCDR) antenna is presented in this paper. This reflectarray antenna consists of a wideband feed and a wideband reflecting surface. The feed is a log-periodic dipole array antenna. The reflecting surface consists of  $26 \times 11$  unit cells. Each cell is composed of a tightly coupled dipole and a delay line. The minimum distance between adjacent cells is 8 mm, which is about  $1/10$  wavelength at the lowest operating frequency. By combining the advantages of reflectarray antennas and those of tightly coupled array antennas, the proposed TCDR antenna achieves ultra-wide bandwidth with reduced complexity and fabrication cost. A method to minimize the phase errors of the wideband reflectarray is also developed and the concept of equivalent distance delay is introduced to design the unit cell elements. To verify the design concept, a prototype operating from 3.4 to 10.6 GHz is simulated and fabricated. Good agreement between simulated and measured results is observed. Within the designed frequency band, the radiation pattern of the TCDR antenna is stable and the main beam of the antenna is not distorted or split. The side lobe levels of the radiation patterns are below  $-11.7$  dB in the entire operating band. It is the first time a tightly coupled reflectarray is reported.

**Index Terms**—Antennas, reflectarrays, tightly coupled arrays, wideband antennas, wideband reflectarrays.

## I. INTRODUCTION

REFLECTARRAY antennas are a hot research topic nowadays [1]. Compared with parabolic reflector antennas, reflectarray antennas are easier to manufacture and have a compact size and a low mass. Moreover, the feed networks of reflectarray antennas are much simpler than those of conventional phased array antennas.

Reflectarray antennas were first proposed and constructed by the waveguide array in 1963 [2]. With the development of printed circuit board technology, many researchers began to use printed patches, dipoles, and slots with different shapes in the design of reflectarray antennas. In [3]–[8], printed

patches were used as unit cells to design reflectarray antennas. The phase of the unit cells reflection coefficient was controlled by adjusting the length of a microstrip line, which was connected to the patch directly. In [9]–[11], printed dipoles with variable lengths were used to design reflectarray antennas. The phase of the unit cells reflection coefficient was controlled by adjusting the length of the dipole. In [12]–[14], patches with variable sizes were chosen as cell elements to construct reflectarray antennas. In [15], slots with varying lengths on the ground plane were used to design reflectarray antennas. In [16], slot antennas with microstrip delay lines were used in the design of reflectarray antennas. In [17], rings with variable rotation angles were employed to construct reflectarray antennas.

Although reflectarray antennas have many advantages compared with parabolic reflector antennas, reflectarray antennas have the problem of narrow bandwidth. This is mainly caused by two factors: the bandwidth of elements on the reflectarray surface and the differential spatial phase delay [18]. Therefore, many researchers have tried to broaden the bandwidth of reflectarray antennas from these two aspects.

In [19] and [20], stacked patches were used as the unit cells of the reflectarray surface to broaden the bandwidth of reflectarray antennas. In [21]–[24], parallel dipoles were employed to enlarge the gain bandwidth of the reflectarray antennas. In [25] and [26], patches with true-time-delay lines were chosen as the radiating elements to broaden the bandwidth of reflectarray antennas. The concept based on artificial impedance surfaces was used to achieve wide gain bandwidth in [27]. In [28] and [29], the subwavelength cells were used to design reflectarray antennas. The distance between adjacent unit cells of conventional reflectarray antennas is approximately half of the wavelength of the center frequency while that distance is less than  $1/3$  wavelength of the center frequency in subwavelength reflectarray antennas. In [30], Bessel filter method was used to design the reflecting surface of the reflectarray antenna. Deng *et al.* [31] combined some of the aforementioned wideband reflectarray design approaches.

In this paper, a novel wideband tightly coupled dipole reflectarray (TCDR) antenna is proposed. The concept of tightly coupled unit cell is introduced into the design of the proposed TCDR antenna. This is inspired by tightly coupled array antennas and connected array antennas [32]–[34]. In tightly coupled arrays and connected arrays, the adjacent cells are placed quite close to enhance the mutual coupling between cells. In connected arrays, even inductors and capacitors are

Manuscript received December 16, 2016; revised August 13, 2017; accepted October 2, 2017. Date of publication December 11, 2017; date of current version February 1, 2018. This work was supported by the U.K. Engineering and Physical Sciences Research Council under Grant EP/N032497/1. (Corresponding author: Wenting Li.)

W. Li, S. Gao, and Q. Luo are with the School of Engineering and Digital Arts, University of Kent, Canterbury CT2 7NT, U.K. (e-mail: wl83@kent.ac.uk; s.gao@kent.ac.uk).

L. Zhang is with the College of Information Engineering, Shenzhen University, Shenzhen 518060, China.

Y. Cai is with the National key Laboratory of Science and Technology on Antennas and Microwaves, Xidian University, Xian 710071, China.

Color versions of one or more of the figures in this paper are available online at <http://ieeexplore.ieee.org>.

Digital Object Identifier 10.1109/TAP.2017.2772311

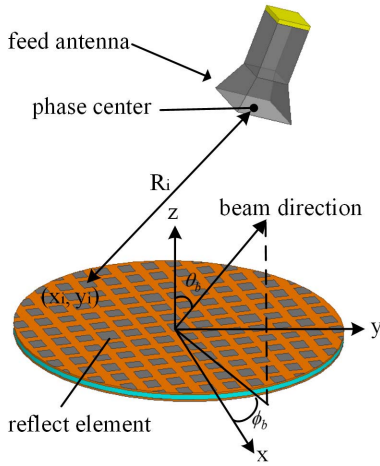


Fig. 1. Configuration of reflectarray antennas.

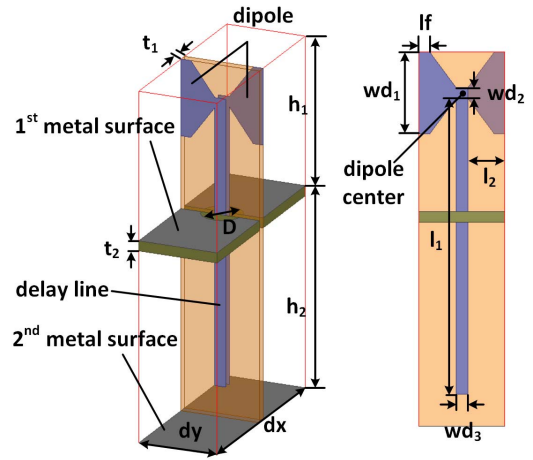


Fig. 2. Side and front views of the proposed element.

added between adjacent cells to enhance the coupling between cells. As reported in [33] and [34], these array antennas have a wide impedance bandwidth. Similarly, the distance between adjacent cells of the TCDR antenna is quite small, which means the coupling between cell elements on the reflectarray surface is strong. So, this type of unit cells has a wide impedance bandwidth, which overcomes the first factor limiting the bandwidth of reflectarray antennas.

As tightly coupled cell elements are used to construct the TCDR antenna, this design combines advantages of tightly coupled arrays and those of conventional reflectarray antennas. As a result, the TCDR antenna has a wide bandwidth with a much simpler feed network compared with tightly coupled arrays, connected arrays, and other UWB direct radiation arrays [35]. In its operating frequency band, the radiation performance of the TCDR antenna is quite stable with reasonable side lobe levels. This paper is organized as follows. The detailed design of TCDR is presented in Section II. Simulated and measured results are given in Section III. Section IV concludes this paper.

## II. TCDR ANTENNA THEORY AND DESIGN

In this section, the concept of equivalent distance delay is introduced to design the required cell elements of the TCDR antenna. Then a TCDR antenna prototype operating from 3.4 to 10.6 GHz is designed. At last, the phase error distribution on the reflectarray surface is discussed.

### A. Equivalent Distance Delay

The configuration of a typical reflectarray antenna is shown in Fig. 1. The required beam direction of the reflectarray is  $(\theta_b, \phi_b)$ . The position of an element on the reflectarray surface is  $(x_i, y_i)$ , and the distance between this element and the phase center of the feed antenna is  $R_i$ . In the following deduction, the phase center of the feed antenna is assumed stable, which means  $R_i$  is frequency independent. According to [18]

$$\Phi(x_i, y_i) = -k_0 \sin \theta_b (x_i \cos \theta_b + y_i \sin \phi_b) + R_i k_0 \quad (1)$$

where  $\Phi(x_i, y_i)$  is the required phase of the reflection coefficient of the reflectarray element, and  $k_0$  is the wave number in the free space. For a reflectarray antenna,  $\Phi(x_i, y_i)$  varies with frequency, even if the beam direction, the positions of the reflectarray elements, and the position of the feed antenna are kept unchanged. In order to eliminate the effects of frequency, (1) is divided by  $k_0$ , then

$$\Phi(x_i, y_i)/k_0 = -\sin \theta_b (x_i \cos \theta_b + y_i \sin \phi_b) + R_i. \quad (2)$$

Let

$$d(x_i, y_i) = \Phi(x_i, y_i)/k_0. \quad (3)$$

Then

$$d(x_i, y_i) = -\sin \theta_b (x_i \cos \theta_b + y_i \sin \phi_b) + R_i. \quad (4)$$

Here  $d(x_i, y_i)$  is called the required equivalent distance delay of a reflectarray element. From the right part of (4), the required equivalent distance delay is determined by the beam direction, the positions of the reflectarray elements, and the position of the feed antenna. It is independent of the frequency. If one reflectarray element is able to keep its equivalent distance delay unchanged in a frequency band, it means the reflectarray element can compensate differential spatial phase delay. In the next section, one of these types of reflectarray elements is introduced.

### B. Design of the Element of the TCDR Antenna

As the bandwidth of elements and differential spatial phase delay result in the bandwidth limitation of reflectarray antennas, two aspects are considered to design the proposed elements of the TCDR antenna. First, tightly coupled dipoles are used to broaden the bandwidth of elements. Second, distance delay lines are used to compensate the spatial phase delay.

The reflectarray element consists of a dipole, a delay line, and two metal surfaces. The side and front views of an element are shown in Fig. 2. The delay line is composed of a pair of parallel microstrips which are connected to the dipole directly. The first metal surface is placed above the second metal surface. The second metal surface is at the bottom of

TABLE I  
PARAMETERS OF THE REFLECTARRAY ELEMENT (UNIT: mm)

$t_1$	$t_2$	$h_1$	$h_2$	$D$	$dy$
0.813	0.813	14.8	20	4	8
$dx$	$wd_1$	$wd_2$	$wd_3$	$lf$	$l_2$
20	7.6	1	1.1	1	3.45

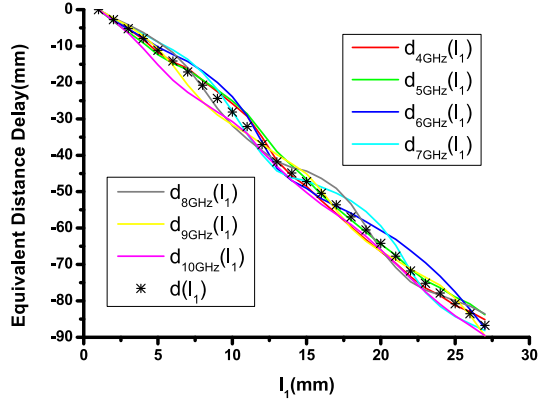


Fig. 3. Equivalent distance delay of the proposed element.

the reflectarray element. The distance between the top of the element and the first metal surface is  $h_1$ , which is critical to the performance of the reflectarray element. It determines the impedance bandwidth. Once the bandwidth of the reflectarray is optimized, the value of  $h_1$  is fixed. However, in some cases, to compensate the spatial phase delay, the required delay line may become very long and the space above the first metal is not enough. In order to accommodate the phase delay lines, a hole is added on the first metal surface. Thus, the delay line can go through the first metal surface via this hole. As the distance between the first metal surface and the second metal surface  $h_2$  is arbitrary, there is no limitation on the length of the delay lines. In this paper,  $h_2$  is 20 mm. The diameter of the hole is  $D$ . The length of the delay line is  $l_1$ .

The dipole and the delay line are printed on both sides of a substrate (Rogers RO4003C), of which the thickness is  $t_1$ . The first metal surface is printed on a substrate (Rogers RO4003C) with the thickness of  $t_2$ . By adjusting  $l_1$ , the equivalent distance delay of the reflectarray element can be controlled. The parameters of the reflectarray element are shown in Table I.

From the results in Table I, it can be seen the minimum distance between adjacent elements is 8 mm. This distance is less than 1/10 wavelength in free space at 3.4 GHz, which is the lowest working frequency in the design. As the distance between two elements is quite small, the coupling between elements is strong as well. So, the element has a very wide impedance bandwidth [32]. It means the element can transfer the energy it receives from the feed antenna to the delay line in a wideband when the reflecting surface is illuminated by the feed antenna. And the delay line used in the design is a true-time-delay line, so it also has wideband performance. Thus, the two factors limiting the bandwidth of a reflectarray are overcome.

The equivalent distance delay that the reflectarray element can offer is shown in Fig. 3. To better demonstrate the

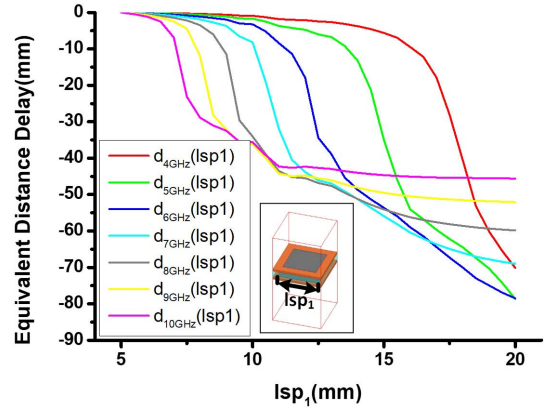


Fig. 4. Equivalent distance delay of the conventional stacked patch.

TABLE II  
PARAMETERS OF THE STACKED PATCH (UNIT: mm)

$tsp$	$dsp$	$lsp2$	$tair$
0.813	21	$0.8 \times lsp1$	3.1

performance of the proposed reflectarray element, the equivalent distance delay that a conventional stacked square patch can offer is also shown in Fig. 4. The equivalent distance delays in Figs. 3 and 4 are calculated from the simulated results in HFSS and (3). The distance between adjacent cells for stacked patch  $dsp$  is set to  $0.49\lambda_0$ .  $\lambda_0$  is the free space wavelength at the center frequency, which is 7 GHz here. The stacked patch is printed on two substrates (Rogers RO4003C) both with the thickness of  $tsp$ . The length of sides of the bottom patch is  $lsp_1$ , and that of the top patch is  $0.8 \times lsp_1$ . Between the substrates is the air gap, whose thickness is  $tair$ . The parameters of the stacked patch are given in Table II.

Let  $d_f(l_1)$  denote the curve of the proposed elements equivalent distance delay versus  $l_1$  at frequency  $f$ , and let  $d_f(lsp_1)$  denote the curve of the stacked patch's equivalent distance delay versus  $lsp_1$  at frequency  $f$ . It can be seen that  $d_f(l_1)$  of the proposed element is more converged than  $d_f(lsp_1)$  of the stacked patch, which means  $d_f(l_1)$  changed much less than  $d_f(lsp_1)$  with frequency changing from 4 to 10 GHz. When  $l_1$  is fixed, although the equivalent distance delays of the proposed element for different frequencies are not the same precisely, they have very small deviations. This means the proposed element can approximately satisfy (4) within a wide frequency band.

Although  $d_f(l_1)$  is quite stable when frequency  $f$  changes, in a certain band, for example, from  $f_1$  to  $f_2$ , it is desirable to find a function  $d(l_1)$  to design the reflectarray, which satisfies the following equation:

$$\sum_{f=f_1}^{f_2} [d(l_1) - d_f(l_1)]^2 = \min. \quad (5)$$

Equation (5) means the sum of squared differences between  $d(l_1)$  and  $d_f(l_1)$  from  $f_1$  to  $f_2$  is minimum. Using  $d(l_1)$  to design the reflectarray results in a more reasonable phase error

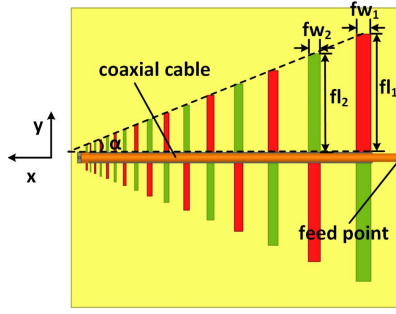


Fig. 5. Configuration of LPDA.

distribution on the reflecting surface for different frequencies. As the left part of (5) is minimum, the derivative of it with respect to  $d(l_1)$  should be zero. Then

$$2 \sum_{f=f_1}^{f_2} [d(l_1) - d_f(l_1)] = 0. \quad (6)$$

Equation (6) can be rewritten as

$$d(l_1) = \sum_{f=f_1}^{f_2} \frac{d_f(l_1)}{N} \quad (7)$$

where  $N$  is the number of frequency points from  $f_1$  to  $f_2$ . In this paper,  $f_1 = 4$  GHz,  $f_2 = 10$  GHz, and  $N = 7$ . In Fig. 3, the curve of  $d(l_1)$  versus  $l_1$  is drawn by asterisk. In the design of TCDR antenna,  $d(l_1)$  is used to calculate the length of delay line for each reflectarray element.

### C. Design of Feed Antenna

As the reflectarray operates from 3.4 to 10.6 GHz, a wideband feed antenna is needed. The log-periodic dipole array (LPDA) which consists of dipoles and a pair of parallel microstrips is chosen as the feed antenna [36]. The dipoles and microstrips are printed on both sides of a substrate (Rogers RO4003C) with the thickness of 0.813 mm. The LPDA is fed by a coaxial cable, of which the outer conductor is connected to one microstrip and the inner pin is soldered to the other microstrip. The configuration of LPDA is shown in Fig. 5. The width of the microstrip is 2.5 mm.  $fl_1 = 29.72$  mm.  $fw_1 = 3.72$  mm.  $\alpha = 21.8$  deg

$$\frac{fl_1}{fl_2} = \frac{fw_1}{fw_2} = 1.2. \quad (8)$$

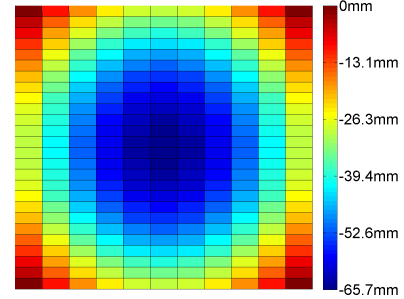
The position of the phase center of the LPDA changes at different frequency points. Let  $p_f(x, y)$  denote the position of the phase center at frequency  $f$ . The coordinates of the phase center at some frequency points are given in Table III. In this design, the position of the phase center  $p(x, y)$  is calculated by using the following equation:

$$p(x, y) = \sum_{f=f_1}^{f_2} \frac{p_f(x, y)}{N} \quad (9)$$

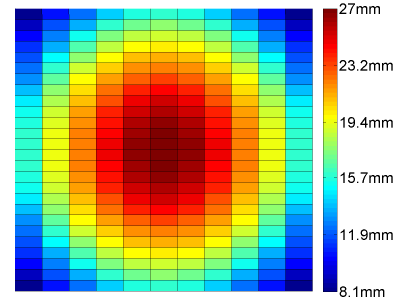
where  $N$  is the number of frequency points from  $f_1$  to  $f_2$ .

TABLE III  
COORDINATES OF PHASE CENTER (UNIT: mm)

Frequency (GHz)	4	5	6	7
$p_f(x, y)$	(-32,0)	(-20,0)	(-11.6,0)	(-7,0)
Frequency (GHz)	8	9	10	
$p_f(x, y)$	(-10.3,0)	(-10.4,0)	(-9.6,0)	



(a)



(b)

Fig. 6. Required (a) equivalent distance delay and (b) length of the delay line for each element on the reflecting surface.

### D. Design of TCDR Antenna

This reflectarray antenna consists of an LPDA as the feed antenna and a reflecting surface. The reflecting surface is composed of  $26 \times 11$  elements. The dimension of reflecting surface is  $210 \times 210 \times 34.8$  mm<sup>3</sup>. The distance between the top of reflecting surface and feed antenna  $Rh_1$  is 97.6 mm. The distance between the phase center of the LPDA and reflecting surface  $Rh_2$  is 119 mm. The required equivalent distance delay for each reflectarray element is calculated according to (4) and is shown in Fig. 6(a). According to the results in Fig. 6(a), the required length of delay line for each element is calculated via  $d(l_1)$  and shown in Fig. 6(b). The configuration of the whole antenna is shown in Fig. 7. In this design, it should be noted that  $R_i$  is the distance between the center of the dipole and the phase center of the LPDA.

### E. Phase Error Distribution and Its Effects on the Side Lobe Level (SLL) of the Reflectarray

Theoretically, to form a focused beam in broadside, the phase on the reflecting surface should be equal after the elements of the reflectarray compensate the spatial phase delay. However, phase errors can exist on the reflecting surface of a reflectarray at some frequency points. As the central frequency



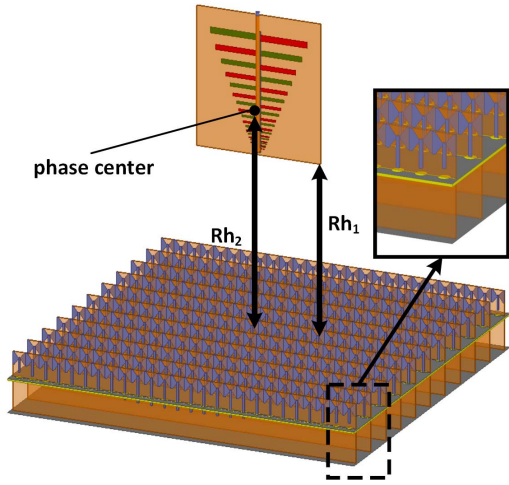


Fig. 7. Configuration of the TCDR antenna.

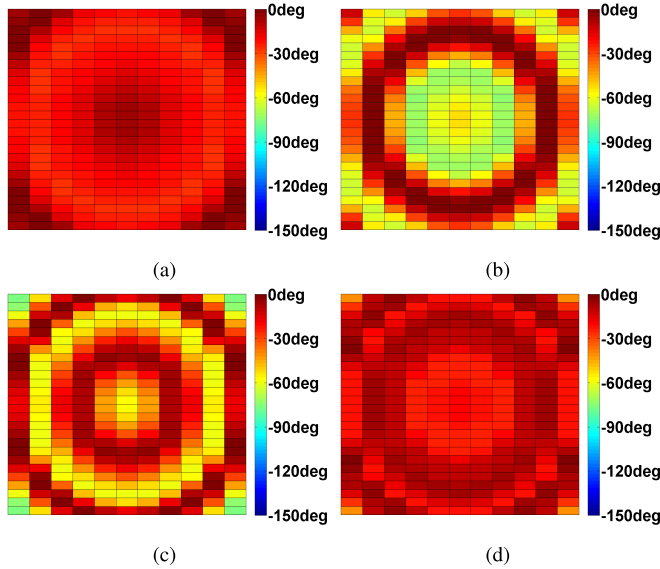


Fig. 8. Phase error distribution at (a) 4, (b) 7, (c) 9, and (d) 10 GHz when  $d(l_1)$  is used to design the reflectarray.

of the reflectarray is about 7 GHz, the phase error distribution based on  $d(l_1)$  is shown in Fig. 8 while that based on  $d_{7\text{GHz}}(l_1)$  is shown in Fig. 9.

In Fig. 8, it can be seen that the worst phase error distribution appears at 9 GHz when  $d(l_1)$  is used to design the reflectarray. At 9 GHz, the largest phase error on the reflecting surface is  $76^\circ$ . However, if  $d_{7\text{GHz}}(l_1)$  is used to design the reflectarray, although no phase error exists on the reflecting surface at 7 GHz, phase error distribution at other frequency points is enlarged. For example, the largest phase error on the reflecting surface at 9 GHz is  $150^\circ$ , which is much larger than that based on  $d(l_1)$  design. Compared with  $d_{7\text{GHz}}(l_1)$ , using  $d(l_1)$  to design the reflectarray minimizes the phase error distribution in a wide frequency range.

As the phase error distribution affects the radiation pattern of the reflectarray, array factors on H-plane at different frequency points are calculated [37] and are shown in Fig. 10.

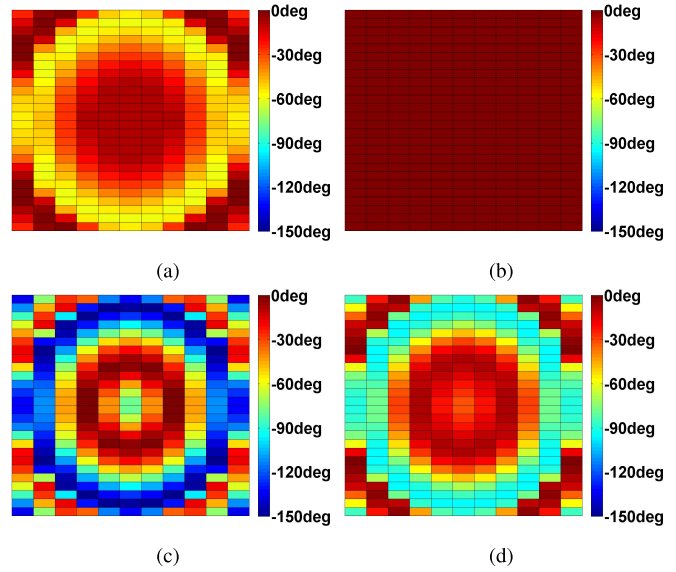


Fig. 9. Phase error distribution at (a) 4, (b) 7, (c) 9, and (d) 10 GHz when  $d_{7\text{GHz}}(l_1)$  is used to design the reflectarray.

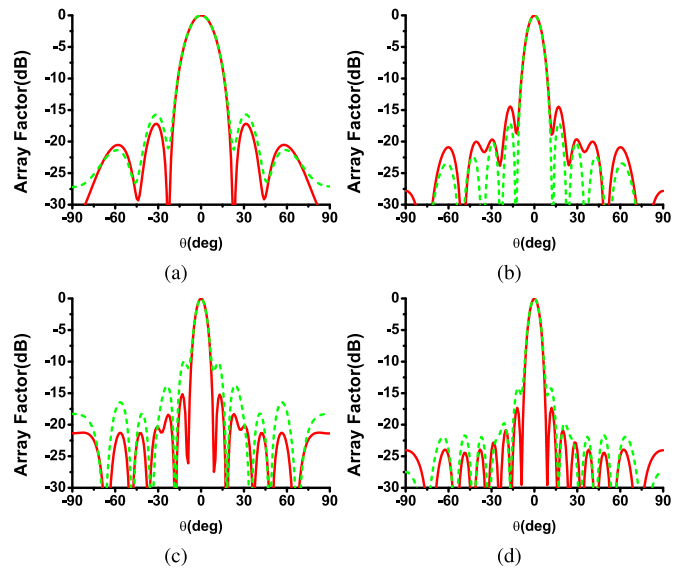


Fig. 10. Array factors at (a) 4, (b) 7, (c) 9, and (d) 10 GHz when  $d(l_1)$  and  $d_{7\text{GHz}}(l_1)$  are used to design the reflectarray, respectively. Solid lines are array factors when  $d(l_1)$  is used. Dashed lines are array factors when  $d_{7\text{GHz}}(l_1)$  is used.

As shown in Fig. 10, different phase error distributions on the reflecting surface result in different first side lobe level (SLL1). Compared with  $d_{7\text{GHz}}(l_1)$ , using  $d(l_1)$  to design the reflectarray decreases the SLL1 within a wide frequency range except slightly increasing the SLL1 at 7 GHz. Especially at 9 GHz, using  $d(l_1)$  decreases the SLL1 by 5 dB.

For the TCDR antenna, its SLL1 is low enough at the central frequency. Compared with SLL1 at the central frequency, TCDR antenna's SLL1 is higher at the lowest and highest operating frequencies. So, slightly increasing the SLL1 at the central frequency would not deteriorate the radiation pattern of the TCDR antenna significantly. Decreasing the SLL1 at lowest and highest operating frequencies will expand the

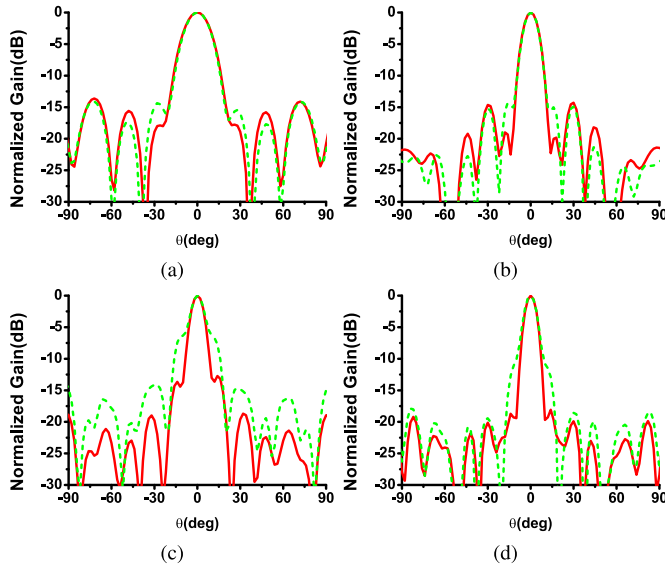


Fig. 11. Simulated radiation patterns at (a) 4, (b) 7, (c) 9, and (d) 10 GHz when  $d(l_1)$  and  $d_{7\text{GHz}}(l_1)$  are used to design the reflectarray, respectively. Solid lines are patterns when  $d(l_1)$  is used. Dashed lines are patterns when  $d_{7\text{GHz}}(l_1)$  is used.

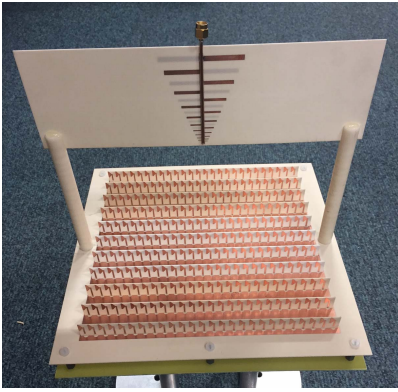


Fig. 12. Photograph of the TCDR.

working bandwidth, in which the TCDR antenna has relatively low SLL. As a result, using  $d(l_1)$  to design the reflectarray can obtain better operating bandwidth than using  $d_{7\text{GHz}}(l_1)$  to design the reflectarray. Fig. 11 shows the simulated radiation patterns of the reflectarray in HFSS when  $d(l_1)$  and  $d_{7\text{GHz}}(l_1)$  are used to design the reflectarray, respectively. Compared with  $d_{7\text{GHz}}(l_1)$ ,  $d(l_1)$  can lead to better SLL of the TCDR antenna.

### III. PROTOTYPE DEVELOPMENT AND SIMULATED AND MEASURED RESULTS

The TCDR antenna is simulated in HFSS. Then, it is fabricated and measured in an anechoic chamber. The photograph of the antenna is shown in Fig. 12. Simulated and measured results are given in this section.

#### A. Radiation Patterns and Reflection Coefficient

As discussed above, the proposed reflectarray element can offer the required equivalent distance delay on the reflecting surface in a wideband. Therefore, one feature of the TCDR antenna is that it can keep its radiation pattern stable in a

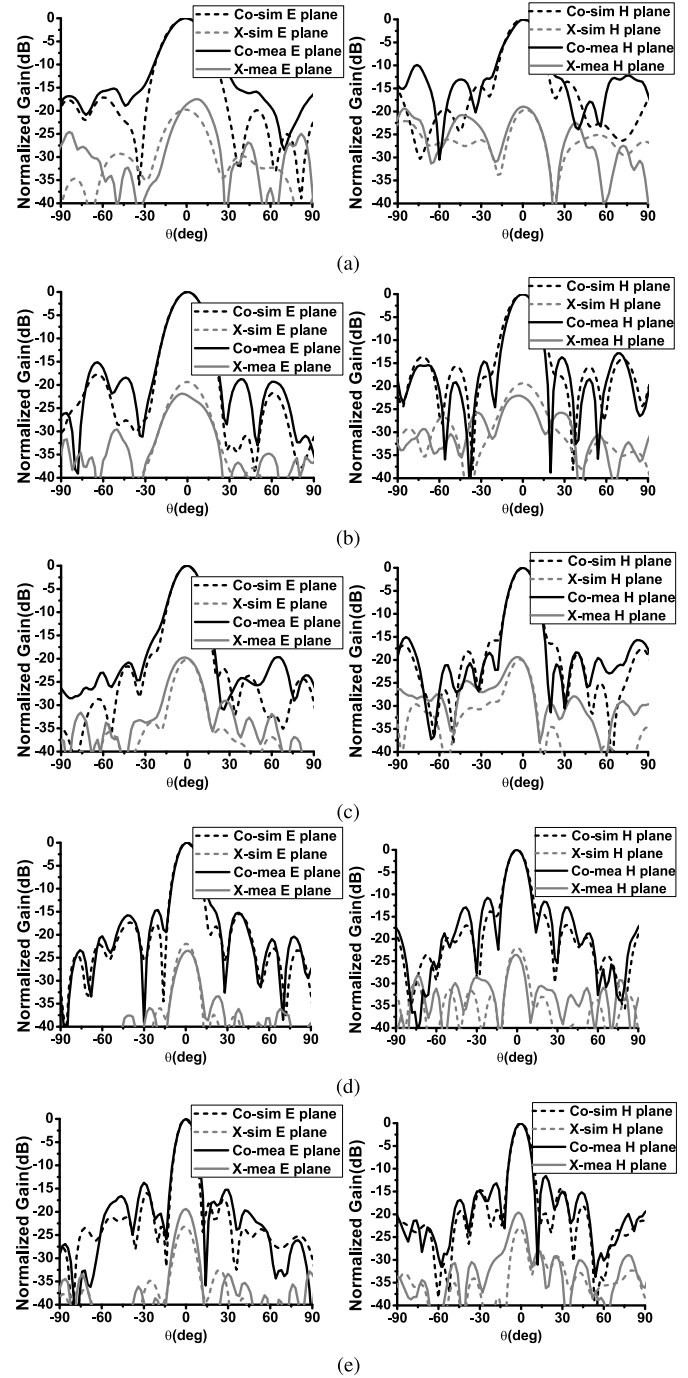


Fig. 13. Radiation patterns of the TCDR. (a) 3.4 GHz. (b) 4 GHz. (c) 5 GHz. (d) 6 GHz. (e) 7 GHz. (f) 8 GHz. (g) 9 GHz. (h) 10 GHz. (i) 10.6 GHz.

large frequency range. The simulated and measured radiation patterns are shown in Fig. 13. Good agreement between the simulated and measured results is observed. From Fig. 13, it can be seen that the radiation pattern performance keeps stable. The shape of the main beam is not distorted with frequency varying from 3.4 to 10.6 GHz. The highest SLL is about  $-11.7$  dB. Fig. 14 shows the 3-D simulated pattern at 7 GHz. Fig. 15 shows the  $|S_{11}|$  of the feed antenna.

Some recent wideband reflectarray antennas reported in the literature and the TCDR antenna in this paper are summarized in Table IV. It should be mentioned that the definition of bandwidth used in those works is not exactly the same. In Table IV,

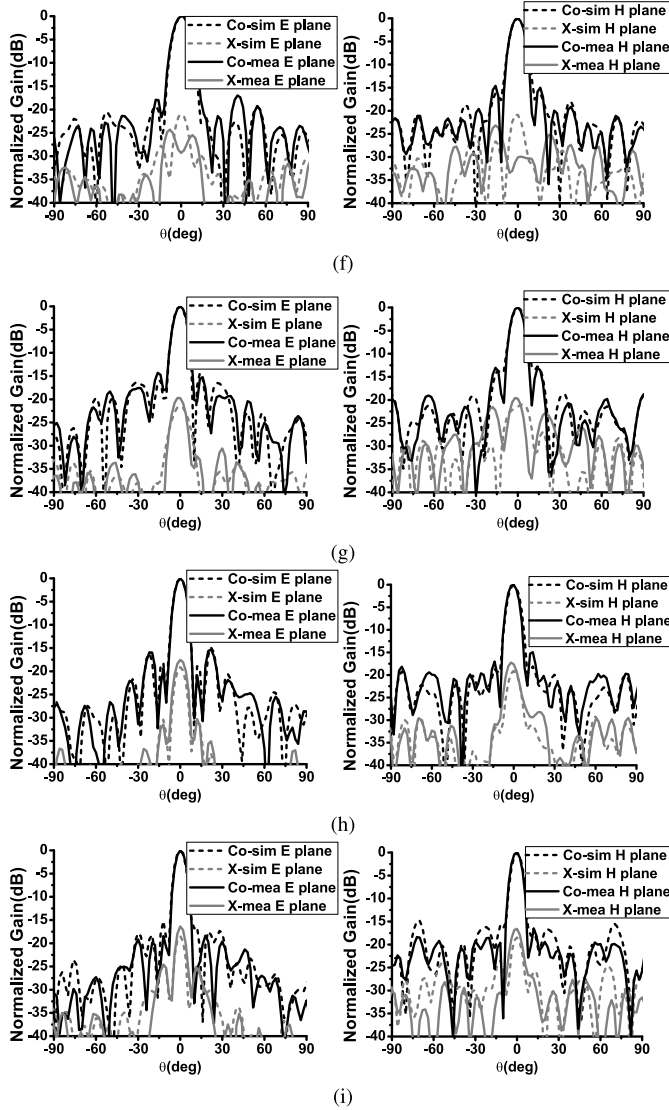


Fig. 13. (Continued.) Radiation patterns of the TCDR. (a) 3.4 GHz. (b) 4 GHz. (c) 5 GHz. (d) 6 GHz. (e) 7 GHz. (f) 8 GHz. (g) 9 GHz. (h) 10 GHz. (i) 10.6 GHz.

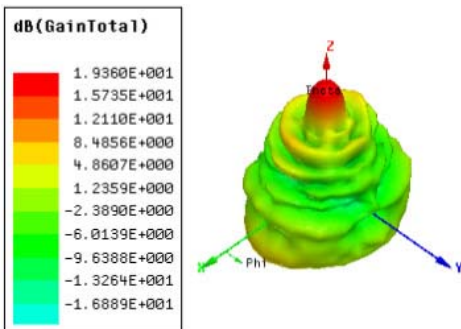


Fig. 14. Simulated 3-D pattern at 7 GHz.

the achieved bandwidths are abstracted by checking whether the antennas have reasonable SLLs and the main beam of the antenna is not distorted.

**B. Gain and Aperture Efficiency**

Fig. 16 shows the simulated and measured gains of the antenna. The simulated gain varies from 12.7 to 21.9 dB in the

TABLE IV  
COMPARISON WITH ANTENNAS IN REFERENCES

Ref. No.	Bandwidth	Max aperture efficiency	Method to achieve wide bandwidth
[30]	2:1	not given	Using Bessel Filters to design element
[31]	1.45:1	78%	Subwavelength spacing & multi-resonance element
[28]	$\leq 1.5:1$	56.5%	Subwavelength element
[21]	$\leq 1.8:1$	64.1%	Using parallel dipoles as element
[19]	1.5:1	not given	True-time-delay element
This paper	3.12:1	38%	Tightly coupled element & true-time-delay line

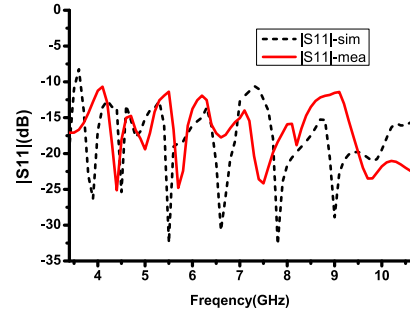


Fig. 15.  $|S_{11}|$  of the feed antenna.

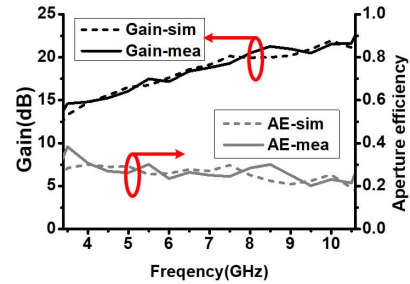


Fig. 16. Simulated and measured gains and AE.

working band and peaks at 10 GHz. The measured gain varies from 13.8 to 22.6 dB and the highest gain appears at 10.6 GHz. The simulated and measured aperture efficiency (AE) of the antenna is also shown in Fig. 16. The simulated AE of the TCDR is over 20% from 3.4 to 10 GHz, and it is larger 17.8% from 10 to 10.6 GHz. The measured AE of the TCDR is over 20% from 3.4 to 10.6 GHz.

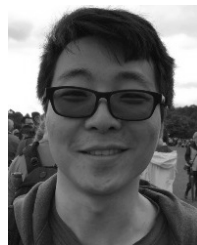
**IV. CONCLUSION**

A novel tightly coupled reflectarray element is proposed in this paper. Using this element, a wideband TCDR antenna is designed and fabricated. The antenna has stable radiation patterns from 3.4 to 10.6 GHz. Over 3:1 frequency range, the main beam of the antenna is not distorted or split with frequency changing. Moreover, the highest side lobe level of the radiation pattern is below -11.7 dB across the band. The antenna is promising for the applications where antennas with wide bandwidth and stable radiation patterns are needed.



## REFERENCES

- [1] W. A. Imbriale, S. Gao, and L. Boccia, *Space Antenna Handbook*. Hoboken, NJ, USA: Wiley, 2012.
- [2] D. Berry, R. Malech, and W. Kennedy, "The reflectarray antenna," *IEEE Trans. Antennas Propag.*, vol. AP-11, no. 6, pp. 645–651, Nov. 1963.
- [3] J. Huang, "Microstrip reflectarray," in *AP-S. Dig. Antennas Propag. Soc. Int. Symp.*, vol. 2, Jun. 1991, pp. 612–615.
- [4] D.-C. Chang and M.-C. Huang, "Multiple-polarization microstrip reflectarray antenna with high efficiency and low cross-polarization," *IEEE Trans. Antennas Propag.*, vol. 43, no. 8, pp. 829–834, Aug. 1995.
- [5] R. D. Javor, X.-D. Wu, and K. Chang, "Beam steering of a microstrip flat reflectarray antenna," in *Proc. IEEE Antennas Propag. Soc. Int. Symp.*, vol. 2, Jun. 1994, pp. 956–959.
- [6] R. D. Javor, X.-D. Wu, and K. Chang, "Design and performance of a microstrip reflectarray antenna," *IEEE Trans. Antennas Propag.*, vol. 43, no. 9, pp. 932–939, Sep. 1995.
- [7] D.-C. Chang and M.-C. Huang, "Microstrip reflectarray antenna with offset feed," *Electron. Lett.*, vol. 28, no. 16, pp. 1489–1491, Jul. 1992.
- [8] K. Chang, "Offset-fed microstrip reflectarray antenna," *Electron. Lett.*, vol. 30, no. 17, pp. 1363–1365, Aug. 1994.
- [9] A. Kelkar, "Flaps: Conformal phased reflecting surfaces," in *Proc. IEEE Nat. Radar Conf.*, Mar. 1991, pp. 58–62.
- [10] D. M. Pozar and S. D. Targonski, "A microstrip reflectarray using crossed dipoles," in *Proc. IEEE Antennas Propag. Soc. Int. Symp.*, vol. 2, Jun. 1998, pp. 1008–1011.
- [11] Y. Chen, L. Chen, H. Wang, X.-T. Gu, and X.-W. Shi, "Dual-band crossed-dipole reflectarray with dual-band frequency selective surface," *IEEE Antennas Wireless Propag. Lett.*, vol. 12, pp. 1157–1160, 2013.
- [12] D. M. Pozar, S. D. Targonski, and H. D. Syrigos, "Design of millimeter wave microstrip reflectarrays," *IEEE Trans. Antennas Propag.*, vol. 45, no. 2, pp. 287–296, Feb. 1997.
- [13] D. M. Pozar and T. A. Metzler, "Analysis of a reflectarray antenna using microstrip patches of variable size," *Electron. Lett.*, vol. 29, no. 8, pp. 657–658, Apr. 1993.
- [14] J. A. Encinar, "Design of a dual frequency reflectarray using microstrip stacked patches of variable size," *Electron. Lett.*, vol. 32, no. 12, pp. 1049–1050, Jun. 1996.
- [15] M. R. Chaharmir, J. Shaker, M. Cubaci, and A. Sebak, "Reflectarray with slots of varying length on ground plane," in *Proc. IEEE Antennas Propag. Soc. Int. Symp.*, vol. 3, Jun. 2002, p. 144.
- [16] Q. Luo *et al.*, "Design and analysis of a reflectarray using slot antenna elements for Ka-band SatCom," *IEEE Trans. Antennas Propag.*, vol. 63, no. 4, pp. 1365–1374, Apr. 2015.
- [17] J. Huang and R. J. Pogorzelski, "A Ka-band microstrip reflectarray with elements having variable rotation angles," *IEEE Trans. Antennas Propag.*, vol. 46, no. 5, pp. 650–656, May 1998.
- [18] J. Huang and J. A. Encinar, *Reflectarray Antennas*. New York, NY, USA: Wiley, 2008.
- [19] S. M. A. M. H. Abadi, K. Ghaemi, and N. Behdad, "Ultra-wideband, true-time-delay reflectarray antennas using ground-plane-backed, miniaturized-element frequency selective surfaces," *IEEE Trans. Antennas Propag.*, vol. 63, no. 2, pp. 534–542, Feb. 2015.
- [20] J. A. Encinar, "Design of two-layer printed reflectarrays using patches of variable size," *IEEE Trans. Antennas Propag.*, vol. 49, no. 10, pp. 1403–1410, 2001.
- [21] J. H. Yoon, Y. J. Yoon, W. S. Lee, and J. H. So, "Broadband microstrip reflectarray with five parallel dipole elements," *IEEE Antennas Wireless Propag. Lett.*, vol. 14, pp. 1109–1112, 2015.
- [22] L. Li *et al.*, "Novel broadband planar reflectarray with parasitic dipoles for wireless communication applications," *IEEE Antennas Wireless Propag. Lett.*, vol. 8, pp. 881–885, 2009.
- [23] R. Florencio, J. A. Encinar, R. R. Boix, and G. Perez-Palomino, "Dual-polarisation reflectarray made of cells with two orthogonal sets of parallel dipoles for bandwidth and cross-polarisation improvement," *IET Microw., Antennas Propag.*, vol. 8, no. 15, pp. 1389–1397, 2014.
- [24] E. Carrasco, M. Barba, J. A. Encinar, M. Arrebola, F. Rossi, and A. Freni, "Design, manufacture and test of a low-cost shaped-beam reflectarray using a single layer of varying-sized printed dipoles," *IEEE Trans. Antennas Propag.*, vol. 61, no. 6, pp. 3077–3085, Jun. 2013.
- [25] E. Carrasco, M. Barba, and J. A. Encinar, "Reflectarray element based on aperture-coupled patches with slots and lines of variable length," *IEEE Trans. Antennas Propag.*, vol. 55, no. 3, pp. 820–825, Mar. 2007.
- [26] E. Carrasco, J. A. Encinar, and M. Barba, "Bandwidth improvement in large reflectarrays by using true-time delay," *IEEE Trans. Antennas Propag.*, vol. 56, no. 8, pp. 2496–2503, Aug. 2008.
- [27] D. M. Pozar, "Wideband reflectarrays using artificial impedance surfaces," *Electron. Lett.*, vol. 43, no. 3, pp. 148–149, Feb. 2007.
- [28] P.-Y. Qin, Y. J. Guo, and A. R. Weily, "Broadband reflectarray antenna using subwavelength elements based on double square meander-line rings," *IEEE Trans. Antennas Propag.*, vol. 64, no. 1, pp. 378–383, Jan. 2016.
- [29] P. Nayeri, F. Yang, and A. Z. Elsherbeni, "Broadband reflectarray antennas using double-layer subwavelength patch elements," *IEEE Antennas Wireless Propag. Lett.*, vol. 9, pp. 1139–1142, 2010.
- [30] L. Liang and S. V. Hum, "Design of a UWB reflectarray as an impedance surface using Bessel filters," *IEEE Trans. Antennas Propag.*, vol. 64, no. 10, pp. 4242–4255, Oct. 2016.
- [31] R. Deng, S. Xu, F. Yang, and M. Li, "A single-layer high-efficiency wideband reflectarray using hybrid design approach," *IEEE Antennas Wireless Propag. Lett.*, vol. 16, pp. 884–887, 2017.
- [32] B. A. Munk, *Finite Antenna Arrays and FSS*. Hoboken, NJ, USA: Wiley, 2003.
- [33] J. P. Doane, K. Sertel, and J. L. Volakis, "A wideband, wide scanning tightly coupled dipole array with integrated balun (TCDA-IB)," *IEEE Trans. Antennas Propag.*, vol. 61, no. 9, pp. 4538–4548, Sep. 2013.
- [34] D. Cavallo, A. Neto, G. Gerini, A. Micco, and V. Galdi, "A 3– to 5-GHz wideband array of connected dipoles with low cross polarization and wide-scan capability," *IEEE Trans. Antennas Propag.*, vol. 61, no. 3, pp. 1148–1154, Mar. 2013.
- [35] F. Zhu *et al.*, "Multiple band-notched UWB antenna with band-rejected elements integrated in the feed line," *IEEE Trans. Antennas Propag.*, vol. 61, no. 8, pp. 3952–3960, Aug. 2013.
- [36] K. Zhang, J. Li, G. Wei, Y. Fan, J. Xu, and S. Gao, "Design and optimization of broadband single-layer reflectarray," in *Proc. Int. Symp. Antennas Propag.*, vol. 2, Oct. 2013, pp. 1226–1229.
- [37] P. Nayeri, A. Z. Elsherbeni, and F. Yang, "Radiation analysis approaches for reflectarray antennas [antenna designer's notebook]," *IEEE Antennas Propag. Mag.*, vol. 55, no. 1, pp. 127–134, Feb. 2013.



**Wenting Li** received the B.S. degree in electronic information engineering and the M.S. degree in electromagnetic field and microwave technology from Northwestern Polytechnical University, Xi'an, China, in 2011 and 2014, respectively. He is currently pursuing the Ph.D. degree with the University of Kent, Canterbury, U.K.

His current research interests include reflectarray antennas, reconfigurable antennas, circularly polarized antennas, and multibeam antennas.



**Steven Gao** (M'01–SM'16) received the Ph.D. degree in microwave engineering from Shanghai University, Shanghai, China, in 1999.

He is currently a Professor and the Chair of RF and microwave engineering with the University of Kent, Canterbury, U.K. His current research interests include smart antennas, phased arrays, satellite antennas, RF/microwave /mm-wave /THz circuits, satellite communications, UWB radars, synthetic-aperture radars, and mobile communications.

**Long Zhang** is currently an Assistant Professor with the College of Information Engineering, Shenzhen University, Shenzhen, China.

**Qi Luo** (S'08–M'12) is a Research Associate with the University of Kent, Canterbury, U.K.

**Yuanming Cai** (M'17) is currently a Lecturer with the National key Laboratory of Science and Technology on Antennas and Microwaves, Xidian University, Xi'an, China.